

SiO production in interstellar shocks^{*}

P. Schilke¹, C.M. Walmsley², G. Pineau des Forêts³, and D.R. Flower⁴

¹ I. Physikalisches Institut der Universität zu Köln, Zùlpicher Str. 77, D-50937 Köln, Germany

² Osservatorio di Arcetri, Largo E. Fermi 5, I-50125 Firenze, Italy

³ DAEC, Observatoire de Paris, F-92195 Meudon Principal Cedex, France

⁴ Physics Department, The University, Durham DH1 3LE, UK

Received 22 April 1996 / Accepted 19 August 1996

Abstract. We study the production of SiO in the gas phase of molecular outflows, through the sputtering of Si-bearing material in grains. The sputtering is driven by neutral particle impact on charged grains in C-type shocks, at the speed corresponding to ambipolar diffusion. Shock speeds in the range $10 < v_s < 40 \text{ km s}^{-1}$ and preshock densities $10^4 < n_H < 10^7 \text{ cm}^{-3}$ have been investigated. Sputtering of Si-bearing material in both the cores and the mantles of the grains is considered. We find that, for v_s of approximately 25 km s^{-1} and n_H of the order 10^5 cm^{-3} , column densities of SiO similar to those observed in molecular outflow regions can be generated by either mechanism. Impact by particles heavier than helium dominates the core-sputtering process for shock velocities of this order. The profiles of rotational transitions of SiO are computed and compared with observations of molecular outflows.

Key words: molecular processes – shock waves – ISM: abundances; jets and outflows; molecules

1. Introduction

Interstellar emission from the CO molecule is observed so extensively in our own and other galaxies that CO has become the accepted tracer of molecular material. On the other hand, emission from SiO, the oxide of the corresponding element in the next row of the Periodic Table, is much less frequently observed, being confined to particular regions, such as molecular outflows. Even allowing for the 10:1 abundance ratio of C:Si, other factors must intervene to account for such a striking difference of behaviour. The explanation is to be found in the depletion of Si from the gas phase, especially in dark molecular clouds (Ziurys et al. 1989), where the depletion of Si is known to be high (several orders of magnitude), while that of C is a more modest factor of 2 or 3 (van Dishoeck et al. 1993). Furthermore, most of the elemental Si is probably to be found in the form of refractory materials, such as silicates, which are difficult to destroy.

Send offprint requests to: G. Pineau des Forêts

^{*} Tables 1 and 2 are available in electronic form at CDS via ftp 130.79.128.5 or <http://cdsweb.u-strasbg.fr/Abstract.html>

Emission from SiO is observed from regions such as molecular outflows and the Galactic centre, which have in common the influence of shocks on their physics and chemistry. In molecular outflows, for example, it is known that SiO lines are broadened and shifted relative to the emission from the ambient gas (Martin-Pintado et al. 1992). It is likely that dynamical effects are responsible for the release of Si, or Si-bearing material, from the grains and into the gas phase. Ultimately, the validity of this conclusion must be established by detailed numerical modelling and comparisons of the model predictions, especially line profiles, with the observations.

Raga, Cabrit and Canto (1995) have published hydrodynamical models of jets from young stars and the molecular outflows to which they give rise. The outflows occur at supersonic speeds and almost certainly generate shocks, probably bow shocks (Davis and Eisloffel 1995). Depending on their velocity and the strength of the magnetic field, these may have C-shock characteristics, at least in their wakes. In the present paper, we present detailed models of the silicon chemistry in such C-shocks and compute the profiles of observable SiO transitions. Our code follows not only the dynamics but also the gas-phase chemistry, as well as interactions with the grains. By these means, the release of Si-bearing material from the grains, its chemical transformation into SiO in the gas phase, and the formation of the lines of SiO and of other observed species can be followed.

We consider two basic cases: (i) the silicon is released from the grain cores, predominantly through impact by particles heavier than He, and then oxidised in the gas phase; (ii) Si-bearing material is released from the grain mantles. By cores, we mean silicate/graphite grains of the type invoked to explain the extinction curve in diffuse gas (see, for example, Draine 1994), and, by mantles, ices of the types indicated by the near-infrared solid-state features (Whittet 1993). Release from cores requires higher impact energies than release from the mantles. The distinction that is made between Si-bearing material in the core and in the mantle may be artificial and is, in any case, uncertain. However, it transpires that the predictions of the model are

much less sensitive to this distinction than was anticipated, for reasons that will become apparent below.

In Sect. 2, we summarize the observations that have been the motivation for the present study. The salient characteristics of the model that we have used, from the dynamical and the chemical standpoints, are presented in Sect. 3. Sect. 4 contains a discussion of the numerical results that relate to cases (i) and (ii) above. Concluding remarks are given in Sect. 5.

2. Observations of the constituents of refractory materials in molecular clouds

It is well established that the constituents of refractory materials, such as silicon, magnesium, calcium and iron, are highly depleted in diffuse interstellar clouds (e.g. Sofia et al. 1994). It is less well established, but nevertheless probable, that the degree of depletion is even greater in dense molecular clouds. This latter statement is based on a number of observations (see Turner 1991 for a review) which we briefly summarize here.

There exist extremely low upper limits to the abundance of SiO in dense, dark clouds, such as TMC1, where it is found that $n(\text{SiO})/n(\text{H}_2) < 3 \times 10^{-12}$ (Ziurys et al. 1989; Martin-Pintado et al. 1992). Given that most gas-phase silicon is expected to be in the form of SiO (Herbst et al. 1989), this suggests that the fraction of silicon in the gas phase is less than about 10^{-7} . By comparison, Sofia et al. (1994) find that, towards diffuse clouds, at least a few percent of the silicon is in the gas phase. The situation appears to be similar for phosphorus-bearing species (Turner 1991). Thus, whilst C, N, O, and S suffer only modest depletion in cold, dense clouds (less than an order of magnitude), it appears that the depletion of Si and P is very large. The same conclusion probably holds for other elements that can be incorporated in refractory materials. For example, Merer et al. (1982) find that, in many galactic sources, $n(\text{FeO})/n(\text{H}_2) < 1 \times 10^{-11}$. Although the fraction of gas-phase iron in the form of FeO in molecular clouds is not well known, their result nonetheless suggests that the depletion of Fe is similar to that of Si.

In some (but not all) interstellar outflows, the SiO abundance appears to be several orders of magnitude larger than in dark clouds. This enhancement is seen most clearly by comparing recent high-quality maps of the SiO distribution around young protostellar bipolar outflows with the intensity distribution in CO and other tracers (see Bachiller et al. 1991; Bachiller and Gomez-Gonzalez 1992; Martin-Pintado et al. 1992; Zhang et al. 1995). As compared to other species, SiO tends to be found at velocities and positions different from those in the ambient medium (see, for example, McMullin et al. 1994; Mundy et al. 1995). Perhaps the most spectacular example is the L1448 outflow (see, for example, Dutrey, Guilloteau and Bachiller 1996), where SiO and CO are observed in "molecular bullets" moving at a projected velocity of roughly 60 km s^{-1} relative to the ambient gas. The SiO/H₂ abundance ratio in this case is estimated to be between 10^{-7} and 10^{-6} in the high velocity gas but less than 10^{-11} in the ambient medium. Thus, the fractional abundance of SiO in the outflow appears to be comparable to the

fractional abundance of Si in diffuse clouds. The most likely explanation is that the silicon, which is incorporated in grains in cold dense clouds, is released from the grains by the action of shocks, which are associated with bipolar outflows. This view is reinforced by the observation, in the same outflows seen in SiO and CO, of emission in the vibrationally excited lines of molecular hydrogen (Davis and Eisloffel 1995), which are thought to be due to shock excitation. In principle, the observed velocity differences provide information on shock velocities. In practice, however, projection effects, and the possibility that the shock does not run into the ambient gas but into pre-accelerated material, render difficult the reliable extraction of this information.

Species other than SiO also exhibit enhanced abundances in outflows. In particular, NH₃ and CH₃OH are observed to have distributions similar to SiO towards the blue lobe of the L1157 outflow (Zhang et al. 1995; Bachiller et al. 1995; Avery and Chiao 1996). Ammonia and methanol are believed to be present in interstellar ices, and their gas-phase abundances are found to be enhanced in the Orion hot core/compact ridge complex (Walmsley and Schilke 1993). It is thought that the ice-mantle material in the Orion hot core has recently evaporated and returned to the gas phase. Thus, it is tempting to conclude that the processes which lead to the release of SiO into the gas phase in molecular outflows are related to those which remove ice mantles in hot cores. However, we note that recent observations with high angular resolution show that SiO is detectable not in the Orion hot core (Chandler and De Pree 1995; Wright et al. 1995) but in the "plateau" or outflow region. A rough estimate, based upon the map of Wright et al., suggests that $n(\text{SiO})/n(\text{H}_2) < 10^{-9}$ in the hot core; this may indicate that silicon is present in the ice mantles as hydrides or as SiO₂, rather than SiO.

A further point of significance is that SiO seems to be absent ($n(\text{SiO})/n(\text{H}_2) < 10^{-10}$) in photon-dominated regions such as the Orion Bar (Jansen et al. 1995). On the other hand, the Si II fine structure line has been detected in the Orion Bar by Haas et al. (1986), who estimated a gas-phase abundance $n_{\text{Si}}/n_{\text{H}} = 3 \times 10^{-6}$. We conclude that silicon may be present in the gas phase of hot molecular (but quiescent) regions in forms other than SiO.

Finally, we note that the "molecular bullets" observed in L1448 and other sources have characteristics similar to the well-known Herbig-Haro objects, associated with jets from pre-main sequence stars. They are also analogous to the "bullets" found by Allen and Burton (1993) to be moving at velocities of the order of 300 km s^{-1} away from Orion IRC2 (see also Tedds et al. 1995). In the latter case, Fe II emission is observed from the apex of the bow shock, and H₂ 2 μm emission from the wake. Iron, like silicon, is a component of refractory materials, and this observation suggests that the grain cores are being destroyed. Furthermore, the width of the Fe II lines implies that H₂ should be collisionally dissociated near the apex of the shock, whereas it is merely vibrationally excited in the wake; this is consistent with the model proposed by Smith and Brand (1990). Similar comments may apply to the shocks in at least some molecular outflows (e.g. L1448).

3. The model

The code that we have used has been adapted from that published by Heck, Flower and Pineau des Forêts (1990) and enables the physical and chemical structure of C-type shocks to be computed. The gas-phase chemical network has been considerably extended to include N-bearing (Pineau des Forêts, Roueff and Flower 1990), S-bearing (Pineau des Forêts et al. 1993), and Si-bearing (Flower et al. 1996) species. In addition, the sputtering of grain mantles (Flower and Pineau des Forêts 1994; Flower, Pineau des Forêts and Walmsley 1995) and of grain cores (Flower and Pineau des Forêts 1995; Flower et al. 1996) has been incorporated in the model. Data on sputtering yields, obtained by means of Monte Carlo simulations of the collisions of atoms with various grain materials (Field et al. 1996), were incorporated as they became available. The initial distributions of the elements C, N, O and S among the different phases of the model are specified in Table 2 of Flower et al. (1995); the distribution of Si is considered below.

3.1. Sputtering of grain cores

A distinction must be made between the sputtering of grain mantles and grain cores. The latter are composed of refractory materials (which we model as solid amorphous SiO₂), with high sputtering thresholds. Significant sputtering of Si by He impact begins when the impact velocity approaches 55 km s⁻¹; heavier particle impact probably extends this lower limit down to about 25 km s⁻¹ (see below). In the model, the impact velocity equates to the ion-neutral velocity difference in the C-shock: the grains are assumed to be charged and to move with the ions, suffering impacts with the neutral species, whose energy increases in proportion to their mass at a given velocity. As the maximum ion-neutral velocity difference increases with the shock speed, high shock speeds are required in order to erode the grain cores. However, C-shocks propagating in dense clouds become dissociative for shock speeds exceeding 60 km s⁻¹ (Flower et al. 1996). It follows that there is a window of shock velocities, between about 25 and 60 km s⁻¹, in which Si atoms may be released into the gas phase, through erosion of the refractory grain cores.

Sputtering by species heavier than He needs to be considered, in spite of their much lower abundance, because their larger mass ensures that the corresponding sputtering thresholds occur at lower impact (and hence shock) velocities (Tielens 1995, private communication). Molecules such as H₂O and CO are amongst the most abundant ‘heavy’ species within the shock, and calculations of the corresponding sputtering yields are required to establish the significance of their contribution to the total sputtering rate. In practice, such calculations are far from trivial, particularly in the near threshold region which is of interest here. Nonetheless, in order to establish the likely role of heavy particle impact, the TRIM simulation code (Ziegler, Biersack and Littmark 1985; Eckstein 1991) has been used to calculate the energy dependence of the sputtering yields following impact by representative heavy particles on solid amorphous SiO₂ (Field et al. 1996). The sputtering yields (for release of Si)

have been fitted as functions of the impact energy E (in eV) by a function of the form.

$$Y(E) = \gamma \exp[-(\beta/E)^\alpha].$$

Although subject to some uncertainty, owing to the approximations inherent in this approach, the computed sputtering yields indicate that heavy particle impact extends the lower limit of the shock velocity, at which significant sputtering of Si occurs, down to about 25 km s⁻¹.

It should be noted that the sputtering thresholds for iron grain-cores are higher, owing to the larger binding energy. The amount of iron liberated in sputtering events cannot be predicted with the present data, but it is likely to be significantly lower than for silicon. Olivine, (Mg,Fe)₂SiO₄, is probably more representative of the composition of interstellar grains than is SiO₂, but the thermodynamical data which are required to calculate, and experimental data with which to compare, the sputtering yields are lacking. Work on determining the sputtering yields for olivine is currently underway and will be reported in a future publication.

3.2. Sputtering of grain mantles

The grain mantles are more readily destroyed than the cores. Draine, Roberge and Dalgarno (1986) showed that substantial erosion of pure H₂O ice mantles can occur in C-shocks with velocities $v_s \geq 25$ km s⁻¹, a result which was essentially confirmed by later work (Flower et al. 1995). If the ice is dirty, or if the substrate is non-polar, molecules tend to be less strongly bound to the grain surface, and even lower shock velocities may be sufficient to cause erosion; this is also the case if heavy particle impact is important.

A related and significant issue is the identity of the products of sputtering. At least at high energies, particle impact on water ice is expected to release atoms or radicals, rather than molecules. At low energies, on the other hand, the incident particle may locally heat the mantle, causing evaporation of H₂O molecules. Minority species, such as SiO₂, are also expected to be ejected as molecules at low impact velocities. As the impact energy increases and approaches about 10 eV, fragmentation can occur, to SiO and O or to Si + O₂. Unfortunately, little is known, either experimentally or theoretically, about the products of sputtering and their variation with the energy of impact. Accordingly, we have made the following assumptions. The rate coefficient (cm³ s⁻¹) for sputtering of Si-bearing species from the mantles of grains of radius a takes the form

$$\pi a^2 \sqrt{\frac{8kT}{\pi m}} 4 \left(1 + \frac{2kT}{E_{th}}\right) \exp \left[-\max \left[\frac{E_{th}}{kT}, \frac{(E_{th} - \frac{3}{2}kT_d)}{kT_n} \right] \right] S,$$

where m is the mass of the incident species, E_{th} is the sputtering threshold energy, and S is the sputtering yield factor. This formula derives from the work of Barlow (1978), who proposed $S = 8 \times 10^{-4}$ for impact by He. In practice, the threshold energy is the major parameter determining the degree of sputtering. For the sputtering of SiO₂ (from the mantle) in molecular form, we

take the threshold energy to be approximately 2 eV, corresponding to the molecule being attached to a polar substrate. On the other hand, for dissociative sputtering yielding $\text{SiO} + \text{O}$, we add the dissociation energy and obtain 6.8 eV for the threshold; when $\text{Si} + \text{O}_2$ are the products, the corresponding threshold energy is 9.9 eV. The reactions that we have included and the parameters that we have used are listed in Table 1 (available only in electronic form).

The ‘temperature’, T , appearing in the above equation for the rate coefficient, is defined in such a way as to take account both of the relative motion of the (charged) grains and the neutrals, responsible for the sputtering, and of the (enhanced) neutral temperature, T_n , in the shock. Specifically, $T = T_d + T_n$, where

$$\frac{3}{2}kT_d = \frac{1}{2}m(v_i - v_n)^2.$$

The argument of the exponential in the expression for the rate coefficient is chosen so as to ensure a sharp fall in the sputtering yield at threshold, expected when ion-neutral drift dominates the sputtering.

Clearly, there is a hierarchy of sputtering processes, determined by their different threshold energies. Depending on the mass of the incident particle, the threshold energies translate into lower limits to the ion-neutral streaming speed at which a given sputtering process becomes significant, as will be seen in Sect. 4 below.

3.3. Dissociation of neutral molecules in collisions with charged grains

A further process which needs to be considered is the dissociation of neutral molecules, including H_2 , in collisions with charged grains within the C-shock. Given the grain-size distribution and the grain: gas mass ratio, it may simply be shown that each molecule of the gas collides with a (charged) grain over the width of the shock, at a speed which is a significant fraction of the shock speed; such collisions are sufficiently energetic to dissociate the molecules.

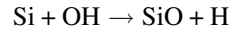
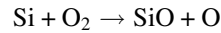
The probability that the molecule is dissociated on impact is not known. In order to investigate the importance of this process, we have assumed that the dissociation probability has an Arrhenius form, $Y_0 \exp(-E_{\text{diss}}/E)$, where E is the impact energy and E_{diss} is the dissociation energy. The multiplicative constant Y_0 has been taken equal to 0.1, which is merely a guess. The collisional dissociation of the more important and abundant species H_2 , CO , O_2 , H_2O and SiO has been incorporated in this way; the data that we adopted are summarized in Table 1. Except for H_2 , which is produced on grain surfaces, all these species reform in the hot shocked gas. The fractional abundance of H can become comparable to that of H_2 within the shock. The width of the shock increases somewhat, owing to the reduced abundance of the dominant coolant, H_2 .

3.4. Gas-phase chemistry of silicon-bearing species

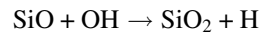
The silicon gas-phase chemistry that we have adopted is presented in Table 2; it derives from the studies of Herbst et al.

(1989), Langer and Glassgold (1990) and MacKay (1995, 1996). Most of the ion-neutral reactions and the corresponding rate coefficients have been extracted from the UMIST ratefile (Millar et al. 1991, 1996). Within shocks propagating in dark clouds, the silicon chemistry is driven mainly by neutral-neutral reactions. The silicon-bearing species are sputtered from the grains (cores or mantles) and enter the gas phase in the form of neutral Si, SiO, SiO_2 , or SiH_4 , depending on the velocity of the shock and the grain-mantle composition in the preshock gas.

If injected directly into the gas phase, Si undergoes oxidation in the reactions



whose rate coefficients have been taken from Langer and Glassgold (1990). In the hot shocked gas, where OH is abundant, the conversion of SiO to SiO_2 proceeds through

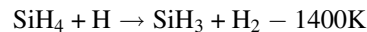


Conversion continues in the cold postshock gas, where OH is produced in the destruction of the water formed in the shock. The rate coefficient for the $\text{SiO}(\text{OH}, \text{H})\text{SiO}_2$ reaction has been given by Langer and Glassgold (1990) as $1.0 \times 10^{-10} \text{cm}^3 \text{s}^{-1}$; this value exceeds that listed by Herbst et al. (1989; $1.0 \times 10^{-11} (T/300)^{0.5} \text{cm}^3 \text{s}^{-1}$), to be found in the UMIST ratefile, by an order of magnitude at $T = 300 \text{K}$. Whilst underlining the uncertainties at low T associated with the existence of small reaction barriers, Herbst (1995, private communication) has suggested that these two values might be reconciled by the expression

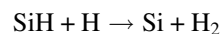
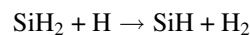
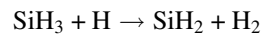
$$k(T) = 1.0 \times 10^{-11} (T/300)^{-0.7} \text{cm}^3 \text{s}^{-1}$$

for the rate coefficient of the reaction $\text{SiO}(\text{OH}, \text{H})\text{SiO}_2$. Along with other molecules, such as H_2O , SiO_2 is subsequently adsorbed on to the grains, becoming a constituent of their mantles.

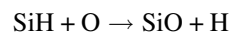
Atomic silicon may be hydrogenated in grain-surface reactions, yielding the saturated species SiH_4 , which enters the gas phase within the shock through sputtering of the mantles. In the hot gas, SiH_4 can undergo the endothermic reaction



which has been studied by Arthur et al. (1989) and Loh and Jasinski (1991); this is followed by the exothermic abstraction reactions



whose rate coefficients have been taken from the compilation of MacKay (1995). Subsequently, the silicon hydrides are converted into SiO by reactions such as



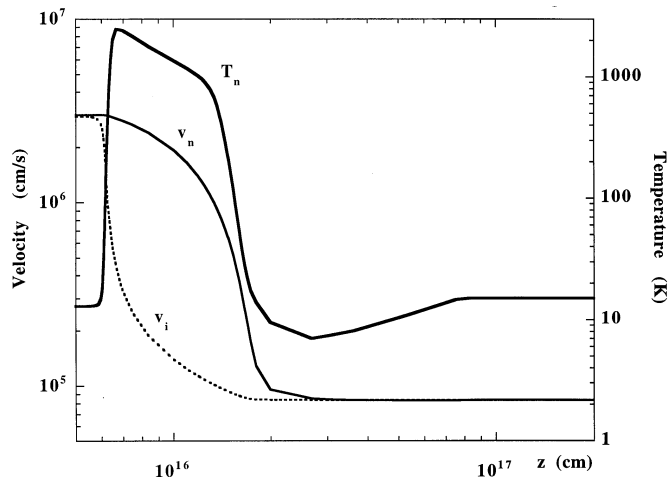


Fig. 1. Velocity and neutral temperature profiles computed for a 30 km s⁻¹ shock; the preshock density $n_{\text{H}} = 10^5 \text{ cm}^{-3}$ and the magnetic induction $B = 200 \mu\text{G}$.

If SiO₂ is injected into the gas phase from the mantles, it is destroyed only slowly, in reactions with He⁺, forming Si⁺ or SiO⁺, which then reacts rapidly with H₂, yielding SiOH⁺ and thence SiO through dissociative recombination (see Table 2).

3.5. Calculation of line profiles

The line profiles were calculated by means of a standard LVG model, using the rate coefficients for collisional transfer between the rotational levels published by Turner et al. (1992). The temperatures, densities and abundances calculated by the shock program were re-binned into 64 bins of fixed velocity width, spanning the entire velocity range from the shock velocity down to zero. In each of these bins, the level populations were calculated using the LVG approximation. The velocity width was taken to be the intrinsic velocity width of a bin plus a turbulent velocity of 2 km s⁻¹. When computing the level populations, the bins were assumed to be non-interacting, but the profiles were calculated by adding the contributions from all bins to the optical depth at a given velocity, assuming a Gaussian line shape. In these calculations, the integration proceeded through the preshock gas and the shock, omitting the post-shock contribution; this was done because our model is not expected to treat events in the postshock gas in a realistic fashion. Since the postshock gas in the model is cold, it would contribute to emission in the low-J transitions only.

4. Results

We shall present results that relate to the sputtering of Si-bearing material from grain cores and from grain mantles. We shall concentrate on models in which the preshock density $n_{\text{H}} = n(\text{H}) + 2n(\text{H}_2) = 10^5 \text{ cm}^{-3}$ and the magnetic induction $B = 200 \mu\text{G}$; the effects of varying these parameters have also been investigated. The fractional abundance of elemental silicon has been taken to be $n(\text{Si})/n_{\text{H}} = 3.6 \times 10^{-5}$ (Anders and Grevesse 1989).

4.1. Sputtering of refractory grain cores

In the present study, we make use of recent calculations of the sputtering probabilities for ion collisions on solid, amorphous SiO₂. The calculations were performed for impact by both He and ‘heavy’ particles, of atomic mass number 12, 16, 28 and 56. In practice, the ‘heavy’ particles are identified with the most abundant species in the shock (C, N, O, CO, N₂, O₂, H₂O), adopting the sputtering yields computed for the mass number closest to the mass of the impacting species. As the impact velocity is the ion-neutral velocity difference in the C-shock, the relative collision energy increases in proportion to the mass of the incident particle. It follows that, in spite of their low abundance, sputtering by heavy particles begins to dominate as the shock velocity decreases.

The velocity and neutral temperature profiles for shock velocity of 30 km s⁻¹ are plotted in Fig. 1; note that the velocities are expressed in the shock frame in this figure, where the shock travels from right to left. The ion and neutral velocities strongly decouple, owing to the low degree of ionization in the gas. This decoupling is resisted by ion-neutral collisions, which result in a kinetic temperature rise in the gas and in the complete erosion of the grain mantles and partial sputtering of the exposed cores. In the models considered here, it has been assumed that the mantles are composed of saturated species such as CH₄, NH₃ and H₂O, which are released in the C-shock; the Si-bearing material (SiO₂) is confined to the grain cores. Nonetheless, it may be seen from Fig. 2 that a substantial fraction (of the order of 10%) of the Si appears in the gas phase, where it is oxidised by O₂ to SiO. The latter is subsequently converted into SiO₂ by the reaction with OH which was discussed in Sect. 3.4. The fractional abundances of O₂, H₂O and OH are also plotted in Fig. 2. The column density of SiO in the shock is large, of the order of 10¹⁵ cm⁻², much higher than predicted by the corresponding model in which sputtering by He impact alone is included. As the main contribution to the column density derives from the gas towards the rear of the shock, practically at the velocity of the postshock gas, the velocity shift between the emission by SiO and by other species, such as CO, which are abundant in the preshock gas, is also predicted to be large, somewhat less than the shock speed of 30 km s⁻¹.

At $v_s = 20 \text{ km s}^{-1}$, the column density of SiO computed in the shock is only of the order of 10¹² cm⁻², compared with 10¹⁵ cm⁻² at $v_s = 30 \text{ km s}^{-1}$. The rapid decrease of the column density of SiO with the shock speed mirrors that of the sputtering probability (for heavy particle impact) as threshold is approached. Although some uncertainty exists in the values of the sputtering yield near threshold, it is clear that erosion of silicate grains, by heavy particle impact, in C-shocks with velocities similar to those considered here can account for column densities of warm SiO similar to those observed in molecular outflows. At $v_s = 30 \text{ km s}^{-1}$, the value of $N(\text{SiO})$ in the shock is in excess of the values that have been deduced from observations of molecular outflows. However, it should be noted that the column densities may have been underestimated in cases where the beam filling factor was low.

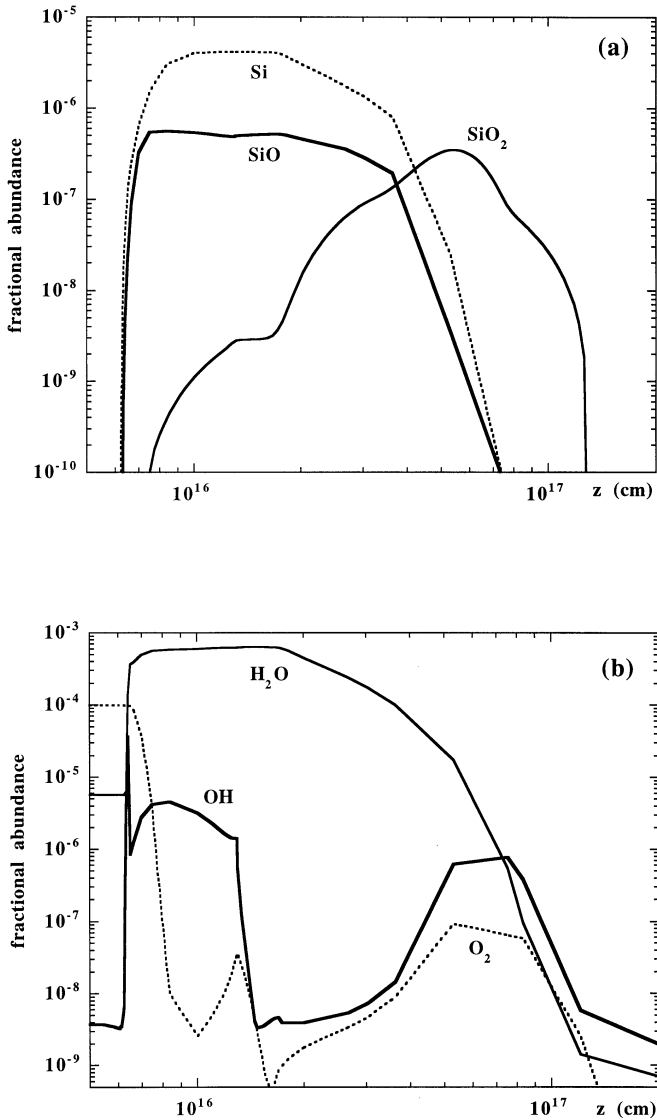


Fig. 2a and b. Fractional abundances, relative to $n_{\text{H}} = n(\text{H}) + 2n(\text{H}_2)$, of **a** Si- and **b** O-bearing species for the same model as in Fig. 1. The elemental Si is confined to the cores of the (charged) grains in the preshock gas and is released into the gas phase, within the shock, through sputtering by heavy neutral species.

A more demanding test of the validity of the model is to be found in a comparison with the observed SiO line profiles. A number of such profiles, for the $J = 2 \rightarrow 1$, $3 \rightarrow 2$ and $5 \rightarrow 4$ transitions, are to be found in the papers of Martín-Pintado et al. (1992) and Bachiller et al. (1991; see Fig. 3a). The velocity profiles of the main beam brightness temperatures are characterized by their asymmetry: a gradual increase with velocity on one side of the maximum, and a more rapid decrease on the other side. As already mentioned, the lines are shifted and broadened relative to the ambient gas, observed in CO and HCO^+ , by amounts that vary considerably from one source to another.

In Fig. 3b are presented specimen SiO rotational line profiles, computed for $v_s = 30 \text{ km s}^{-1}$, using the LVG approximation. As in the previous figures, the velocity is expressed in the

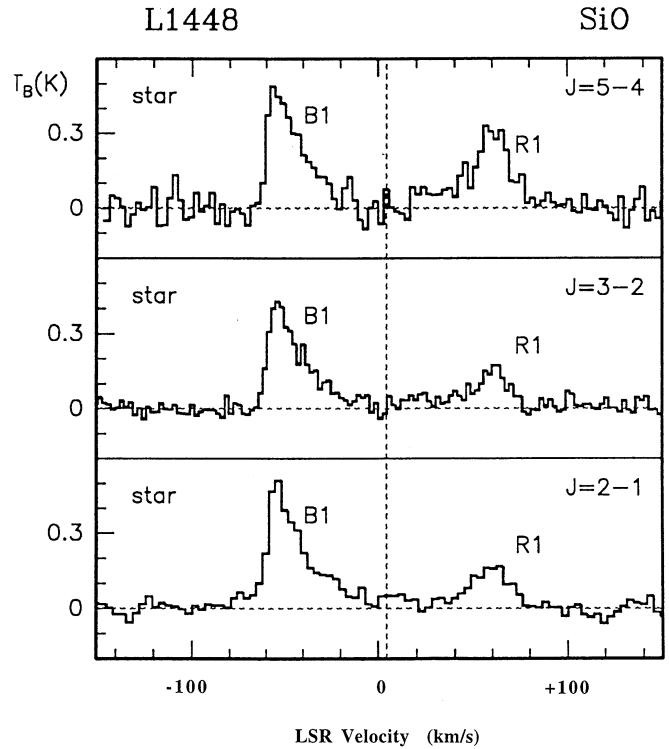


Fig. 3. **a** SiO rotational line profiles observed in L1448 by Bachiller et al. (1991). The red and blue lobes are indicated by ‘R’ and ‘B’, respectively.

shock frame, and the preshock gas is to the right and the postshock gas to the left in Fig. 3b. The line of sight is assumed to be parallel to the direction of propagation of the shock.

It may be seen in Fig. 2 that the fractional abundance of SiO increases rapidly within the shock, and the corresponding rise in the brightness temperature is evident in Fig. 3b. The optical depths in the lines are significant, increasingly so for the transitions to the more highly populated J-levels. The populations depend on radiative and collisional transfer within the shock and have been calculated simultaneously with the shock structure (see Sect. 3.5). In the postshock gas, the computed velocity gradient tends to zero, and the LVG approximation becomes invalid. In view of the uncertainties in the beam filling factors, greater weight should be attached to the relative than to the absolute line intensities.

It transpires that there is considerable overlap between the line intensities predicted for the two cases of mantle and core erosion. When $v_s = 25 \text{ km s}^{-1}$, the integrated line intensities are of the order of those observed, with the latter showing significant variation from source to source. The line intensities become too weak, compared with the observations, for $v_s < 20 \text{ km s}^{-1}$, and too strong for $v_s > 30 \text{ km s}^{-1}$. In view of the current uncertainties in the sputtering yields and products, from both the mantles and the cores, these limits should be taken as indicative.

4.2. Sputtering of Si-bearing material in grain mantles

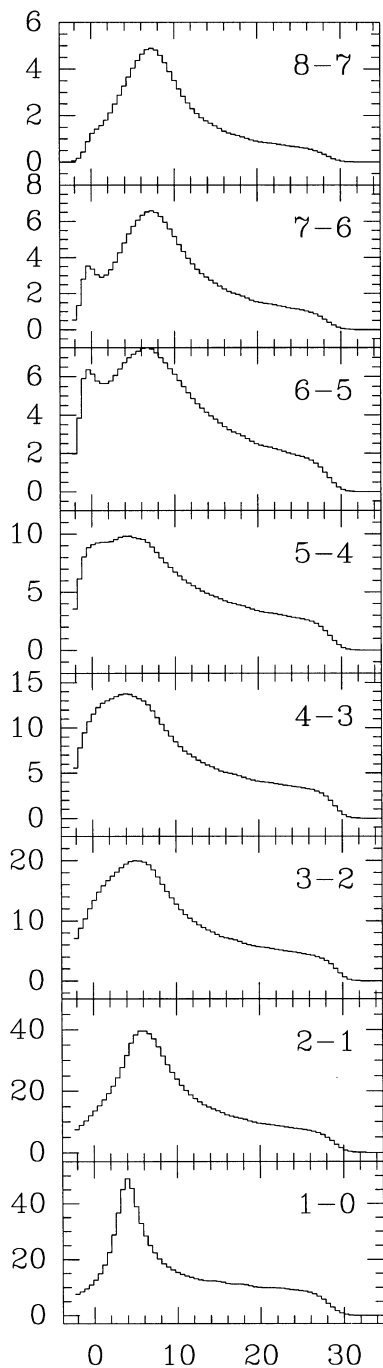


Fig. 3. b Synthetic SiO line profiles for the model shown in Fig. 1, computed using an LVG approximation. The main beam brightness temperature (K) is plotted against the velocity (km s^{-1}) in the shock frame, where the preshock gas has the highest and the postshock gas the lowest velocity.

We consider three scenarios for grain-mantle sputtering, which differ in the form in which silicon is assumed to be present on the grain surface: SiO, SiO₂, or SiH₄. The first option corresponds to the extreme case in which SiO is available directly. The second option generates a self-consistent model, since SiO in the post-shock is converted into SiO₂ and deposited on grain mantles in this form. It is also conceivable that SiO, if deposited directly, reacts with the oxygen in the amorphous water ice and forms SiO₂ on the surface. The third option follows the assumption made in many studies of grain-surface chemistry (e.g. MacKay 1995), namely that hydrogenation occurs very quickly, yielding SiH₄ on the grain surface. We shall present "standard models" for these three hypotheses, with $v_s = 30 \text{ km s}^{-1}$ (which corresponds to a maximum velocity difference between molecules and grains of approximately 25 km s^{-1}), $n_H = 10^5 \text{ cm}^{-3}$ and $B = 200 \mu\text{G}$ initially. The relevant physical and chemical processes are discussed in the context of these standard models. We then make the assumption that silicon on grain surfaces is to be found in the form of SiO₂ and vary the shock velocity and preshock density in order to investigate the variations in the SiO column densities and line intensities. To facilitate comparison with the observations, we calculate SiO line profiles, introducing the temperature, abundance and velocity profiles of the shock in an LVG program (Sect. 3.5).

Another choice which has to be made is of the binding energies of the molecules to the mantle. The critical velocity for grain mantle removal is approximately 10 km s^{-1} for a non-polar and 20 km s^{-1} for a polar substrate, assuming the sputtering thresholds to be 0.7 eV and 2.1 eV, respectively, or four times the typical binding energies (Pirronello 1993). It is unclear which values of the binding energy are appropriate in our cases. Although pure SiO, SiO₂ and SiH₄ have low intrinsic binding energies, they could be present in a polar H₂O matrix. Since it turns out that (except for direct release of SiO) the critical velocity for SiO production is determined by processes other than simple mantle removal, we adopt 'polar' binding in all the models.

The percentage of silicon present in the mantle is also a free parameter, although it should not be larger than the gas-phase abundance of silicon in diffuse clouds (Sofia et al. 1994). The SiO abundance derived from the observations (Martin-Pintado et al. 1992) is consistent with up to a few percent of the silicon having been released into the gas phase. We have assumed that 1% of the interstellar silicon is present in the grain mantles.

The molecular abundances as functions of the distance are shown in Fig. 4 for the three scenarios that we are considering. Since the three cases differ only in relation to minor species, the temperature and velocity structure and the abundances of the major molecules are essentially the same. In Fig. 4, we display the abundances of SiO, SiO₂ and SiH₄, and of the oxygen-bearing species OH and H₂O.

In all the models, the mantles are rapidly and completely destroyed in the shock, and the silicon in the mantles is transferred to the gas phase. The oxygen chemistry is such that atomic

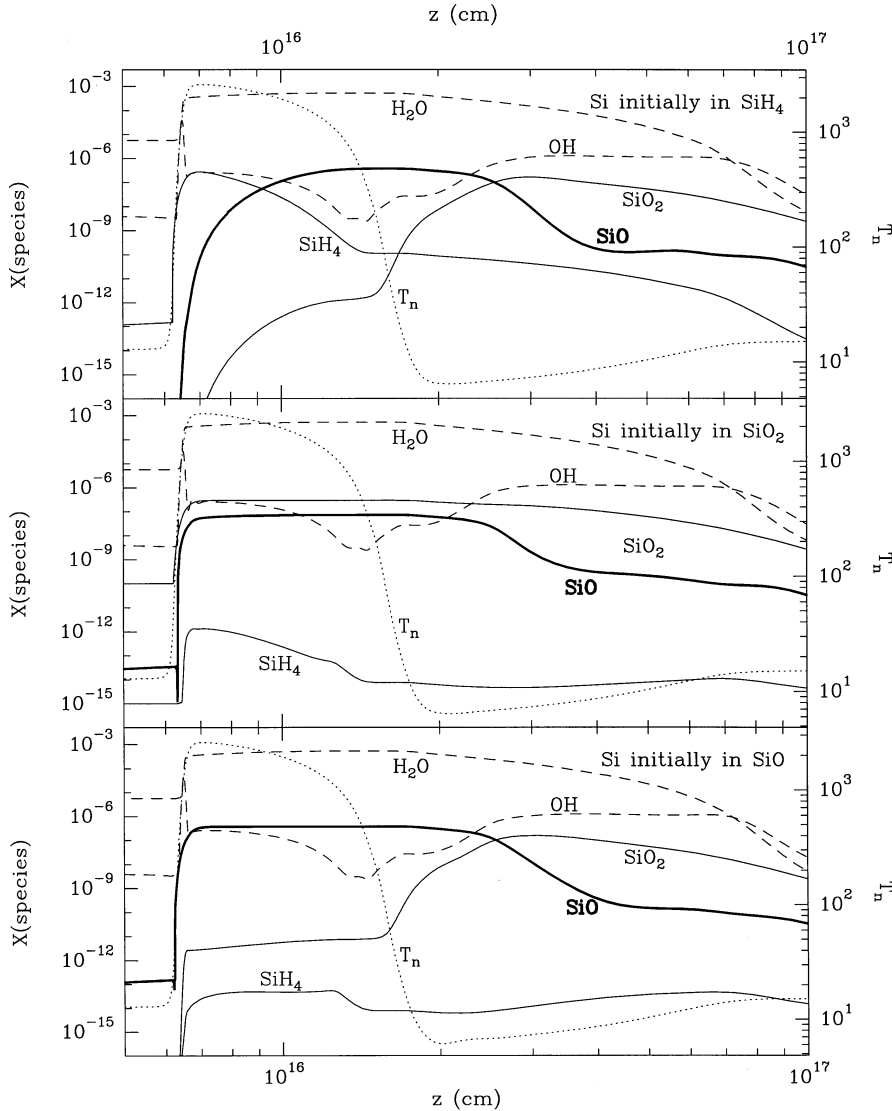


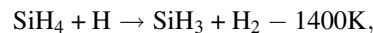
Fig. 4. Molecular abundances through the shock computed under the assumption that silicon-bearing material is released into the gas phase from the grain mantles. **a** Si initially in the form of SiO (bottom); **b** Si initially in the form of SiO₂ (centre); and **c** Si initially in the form of SiH₄ (top). The neutral temperature profile is also shown.

oxygen is almost immediately transformed into H₂O, which becomes the dominant oxygen-bearing species. After the passage of the shock wave, H₂O is lost from the gas phase, partly through accretion on to grains, and partly through its conversion (by ion-molecule reactions) into OH, whose fractional abundance attains 10⁻⁶ in the post-shock gas. Once abundant in the gas phase, OH converts SiO into SiO₂. Both SiO and SiO₂ are subsequently accreted on to the grains. This ‘postshock’ chemistry is the same in all the models. We emphasize that the chemistry in the postshock gas is very different from that in the gas phase of cold clouds because of the much enhanced abundance of the very reactive OH radical. If adsorption processes are neglected, then SiO₂ is eventually destroyed in reactions with atomic ions, and SiO becomes the main silicon-bearing species, as predicted by models of the gas-phase chemistry in dark clouds (Herbst et al. 1989).

The situation differs if silicon is initially in the form of SiO₂, rather than SiO. The mantles are once again destroyed rapidly and completely, but SiO₂ is a stable molecule which, in the gas

phase, is removed only by reactions with atomic ions, whose abundance is low. The only mechanism which destroys SiO₂ reasonably fast is dissociative sputtering which, as mentioned above, has thresholds of 6.8 and 9.9 eV; these are intermediate between the thresholds for removal of a polar mantle (2.1 eV) and erosion of the core (about 40 eV). In the standard model, the efficiency of conversion to SiO, of silicon initially in the form of SiO₂, is only about 20% with the parameters that we have employed.

The species SiH₄ is a saturated and stable molecule, although not quite as stable as SiO₂. We have already seen that, in the hot gas, it can be destroyed by atomic hydrogen,



and subsequent reactions with H yield SiH₃, SiH₂, and SiH, which reacts with O, forming SiO. Low energy shocks may release SiH₄ from the mantle but not destroy it, since the temperature remains too low. Apart from the activation energy of the initial reaction, the factor limiting the reaction chain is the

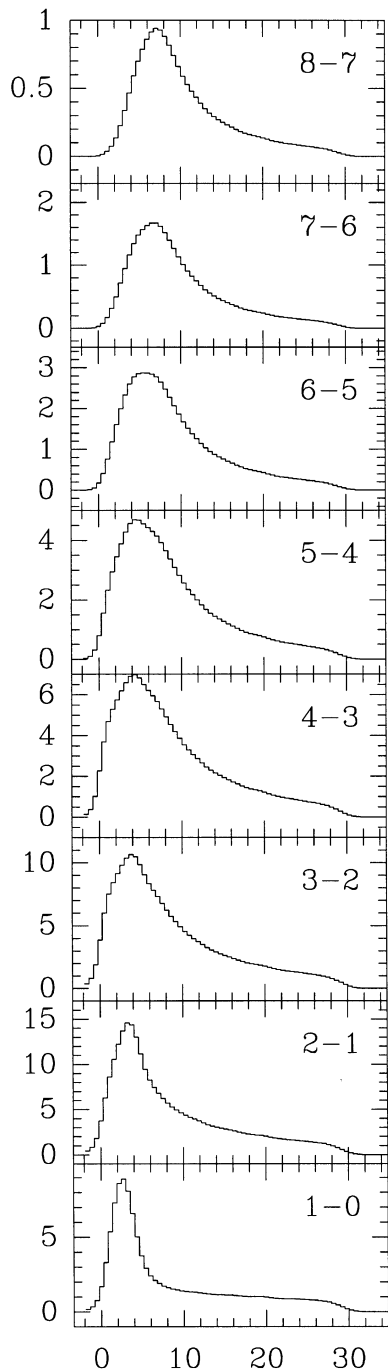
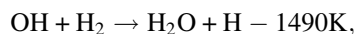


Fig. 5. As Fig. 3, but for the case of mantle sputtering (reference model, Si initially in the form of SiO₂; see Fig. 4, centre).

availability of atomic hydrogen, which is produced in the formation of water,



and in the dissociative sputtering of H₂, mentioned above. In low energy shocks, SiH₄ would be released from the mantles, remain (unseen) in the gas phase without being converted into

SiO, and be re-accreted on to grains in the postshock gas. Even if the shock is sufficiently energetic to destroy SiH₄, the SiO forms only gradually, although eventually most of the SiH₄ is transformed into SiO. As in the case where SiO₂ is assumed to be the dominant silicon-bearing species in the mantle, dissociative sputtering enables Si to be released into the gas phase, where it is converted rapidly into SiO. However, the bulk of the SiO in the gas phase is still produced through the destruction of SiH₄.

As an illustration of the results, we show the calculated line profiles for our standard model (SiO₂ option; see Fig. 5). The velocities are expressed in the shock frame in which the preshock gas flows at the shock velocity (30 km s⁻¹ in this case). The thermal energy required to excite the higher levels is available only in the vicinity of the temperature maximum, while the lower levels can also be excited toward the back of the shock, where the temperature is lower. Consequently, the peak velocity is very close to the postshock velocity for the lower levels but is shifted towards the preshock velocity for the higher levels; a tail towards the preshock velocity is also present for the lower excitation lines. In outflow sources, one would expect both a red- and a blue-shifted emission peak, the line profiles being steepest towards the largest velocity offset, with a wing towards, but no emission at, the ambient velocity. However, when comparing with observations, one has to bear in mind that geometric effects, associated with departures from a plane-parallel shock front, and projection effects will conspire to make this signature less identifiable.

Of the sources that have been observed, L1448 seems to be an outflow which is reasonably well approximated by plane-parallel shocks, since the observations (Bachiller et al. 1991; Fig. 3a) and calculations (Figs. 3b and 5) are in good agreement. Not only is the SiO emission peak displaced from the ambient velocity, but also the general line shape is correctly predicted: steep towards the highest velocities with a wing pointing towards the ambient velocity. The CO line shapes are similar, but, in this case, there is a pronounced ambient component. It may seem embarrassing that, in this source, the velocity difference between the "bullets" and the ambient medium is about 65 km s⁻¹, in excess of that possible for a C-shock. However, it must be borne in mind that this velocity difference is not equal to the shock velocity, which could be higher owing to projection effects or lower if the shock propagates into a medium which has been pre-accelerated by winds or previous shocks (see Dutrey et al. 1996 for a discussion). It is well known that outflows are not continuous processes, but consist frequently of "bullets" ejected with wide intervals between them. For example, the observations of Zhang et al. (1995) show the SiO emission in L1157 to be in front of the working surface of the shock, which is delineated by the H₂ emission. It is probable that the current shock propagates into an SiO-rich cloud which has been pre-processed by an earlier shock.

The integrated rotational line intensities, for various shock velocities and densities, are shown in Fig. 6. When comparing with observations, it must be recalled that these values were calculated assuming a particular geometry (plane-parallel and face-on) and a constant preshock density and magnetic field.

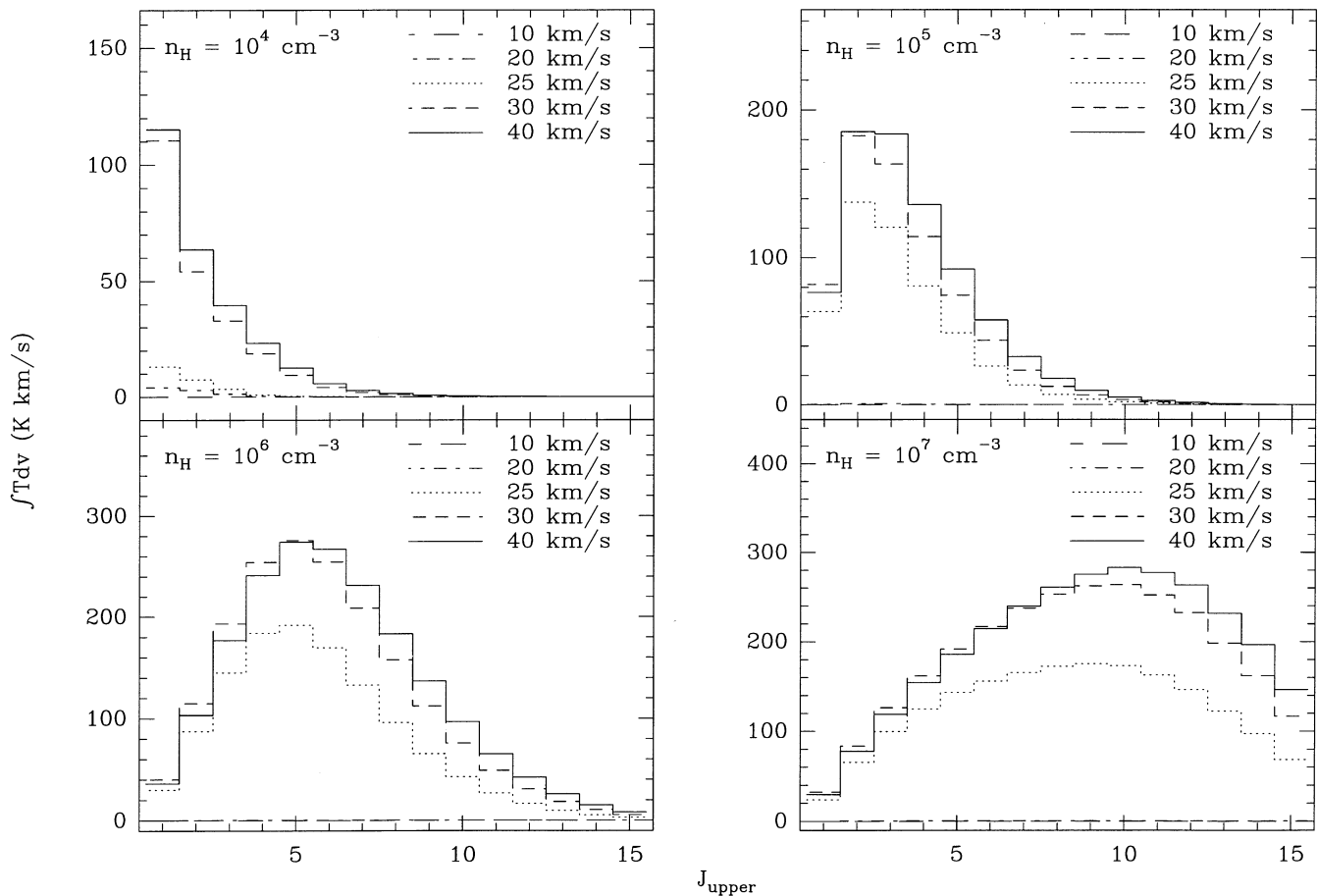


Fig. 6. Integrated intensities of SiO transitions. Four panels are shown, one for each preshock density considered: 10^4 , 10^5 , 10^6 and 10^7 cm^{-3} . In each panel are displayed histograms of the integrated intensities for the five shock velocities considered: 10, 20, 25, 30 and 40 km s^{-1} . Note that the intensities for 10 and 20 km s^{-1} are generally too low to be apparent.

Any possible postshock contribution is neglected, and a beam filling factor of unity is adopted. Moreover, the absolute intensities can be scaled up or down with the amount of silicon assumed to be available in the grain mantles, although the scaling is not linear, because of optical depth effects (the maximum optical depths in our reference model are of order 1). In spite of these restrictions, we believe that the observed line intensities can be used, in conjunction with the predictions of the model, to estimate the shock speed and the gas density.

The critical velocity for SiO production is sharply defined (see Fig. 6): whilst the line intensities are negligible at a shock velocity of 20 km s^{-1} , a 25 km s^{-1} shock already gives rise to strong SiO emission. The density dependence of the critical velocity is weak, but, at the lowest density considered, a 30 km s^{-1} shock is required to produce observable emission. Above this critical value, the velocity dependence is also weak. Thus, the differences between the results for $v_s = 30 \text{ km s}^{-1}$ and 40 km s^{-1} are practically negligible and probably attributable to variations in the maximum temperature and compression factor. The higher the shock velocity, the higher the J -value at which the intensity peaks. The density determines the strongest transition: preshock densities of 10^4 , 10^5 , 10^6 and 10^7 cm^{-3} peak

at $J_{\text{upper}} = 1, 3, 6$ and 10 , respectively; this behaviour is determined by the relative values of the rates of radiative and collisional de-excitation. A different representation of the results is to be found in Fig. 7.

Of what use then is SiO as a diagnostic of shocks? From what has been said above, it is apparent that, if SiO is seen at all, the shock velocity must exceed about 20 km s^{-1} . However, it is difficult to say by how much because the absolute intensities are uncertain, owing to the unknown amount of silicon initially available in the mantles. This quantity will, in general, depend on the history of the cloud. The line ratios, by virtue of the large dipole moment of SiO, are good density indicators. The advantage of SiO in this respect is that it traces only the shocked gas, while other density indicators are confused by emission from the ambient material. Sub-millimetre receivers have recently become available that are capable of observing the $8 \rightarrow 7$ line, which will prove to be very useful for determining the densities in the shocks associated with molecular outflows.

We close this section with a brief discussion of the possible importance of heavy particle impact in removing the grain mantles. We have included this process in a few of our calculations, under the assumption that the sputtering probability

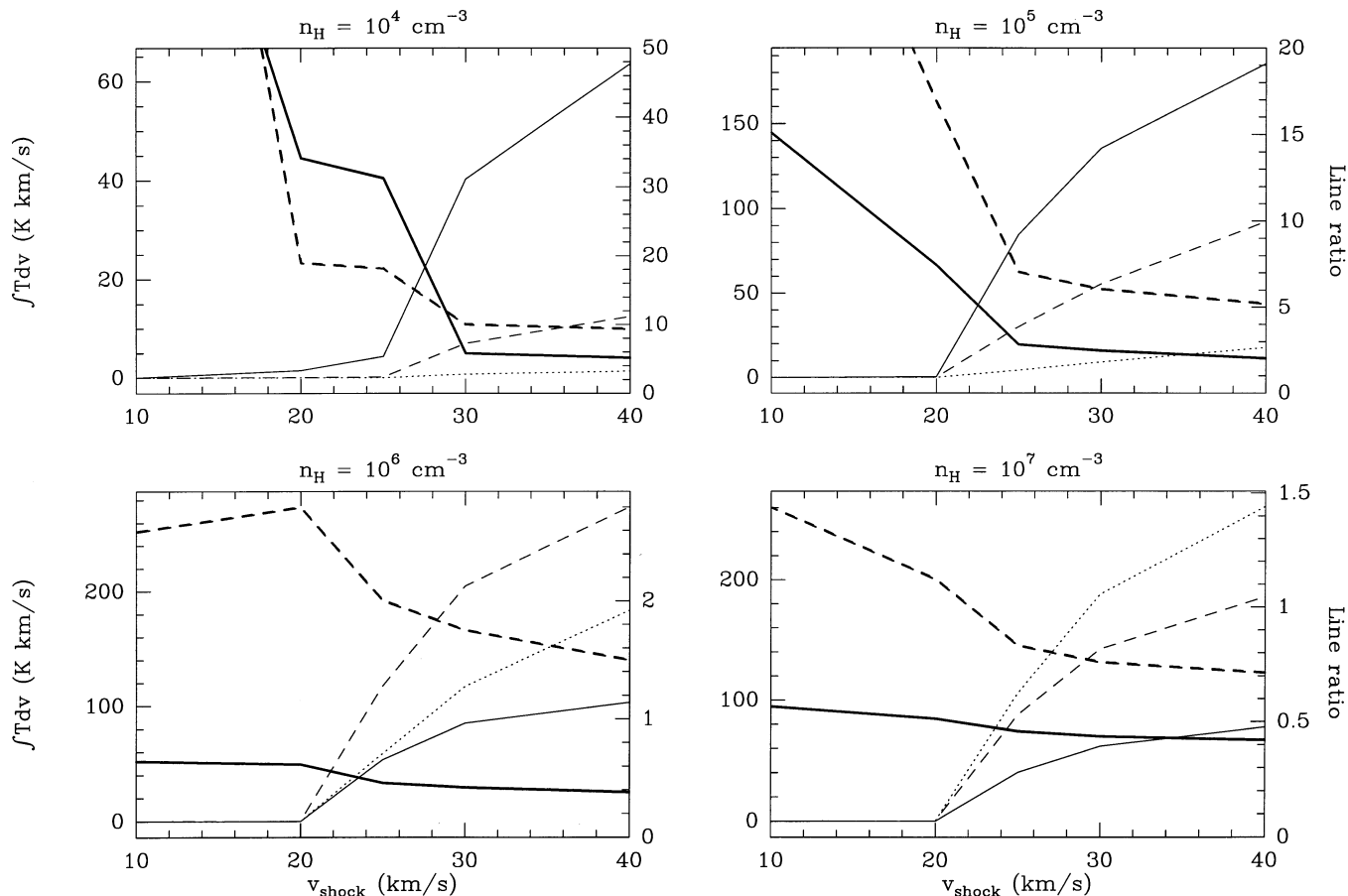


Fig. 7. Integrated intensities and line ratios of selected transitions for different densities as function of shock velocity for the standard model. We show the integrated intensities of SiO(2-1) (light solid line), SiO(5-4) (light dashed), SiO(8-7) (light dot ted) and line ratios of SiO(2-1)/SiO(5-4) (heavy solid) and SiO(8-7)/SiO(5-4) (heavy dashed). The left and right axes denote the integrated intensity and the line ratios, respectively.

depends only on the energy, and not on the mass, of the impacting species; calculations have shown this to be approximately true for the sputtering of refractory material (SiO_2) in grain cores (Field et al. 1996). In Fig. 8 are presented the values of the brightness temperature of the $2 \rightarrow 1$ transition of SiO, integrated with respect to velocity, for a range of shock velocities, computed with and without heavy particle sputtering. The corresponding results for the sputtering of the grain cores, including heavy particle impact, are shown for comparison.

It will be seen that heavy particle impact on the mantles becomes significant at low shock speeds, $v_s < 25 \text{ km s}^{-1}$, as might have been anticipated; even at $v_s = 15 \text{ km s}^{-1}$, significant SiO emission is predicted when heavy particle sputtering is included. For shock speeds in excess of 25 km s^{-1} , heavy particle sputtering of the core is dominant. Perhaps the most striking feature of Fig. 8 is the similarity of the results that have been obtained under quite different assumptions.

5. Concluding remarks

Given the large enhancement of gas-phase silicon observed in molecular outflows and the existence of shocks in such regions, it is reasonable to suppose that the two phenomena are related.

In practice, bow shocks are likely to occur, exhibiting C-shock characteristics in their wakes. In these zones, ambipolar diffusion results in the neutral atoms and molecules drifting relative to the predominantly charged grains at velocities which are comparable with the shock velocity.

In the range of shock velocities that we have investigated ($10 < v_s < 40 \text{ km s}^{-1}$), it is clear that the grain mantles are readily and completely destroyed; any silicon present in the mantles reappears in the gas phase. If the silicon is injected into the gas in the form of Si or SiO, SiO line emission may be expected from the hot, shocked medium; further oxidation, to SiO_2 , occurs in the postshock gas. However, if SiO_2 or SiH_4 is released from the grains, the gas-phase chemistry struggles to produce sufficient SiO to be observable. Dissociation of these molecules accompanying their sputtering then seems to be the only reasonable way of accounting for the observed line intensities, but higher shock speeds are required to initiate this ‘dissociative sputtering’ process. Indeed, the requisite shock speeds become comparable to those necessary to destroy amorphous SiO_2 in the refractory grain cores, through heavy particle impact.

It is probable that impact by relatively abundant species that are heavier than helium dominates the sputtering process at low

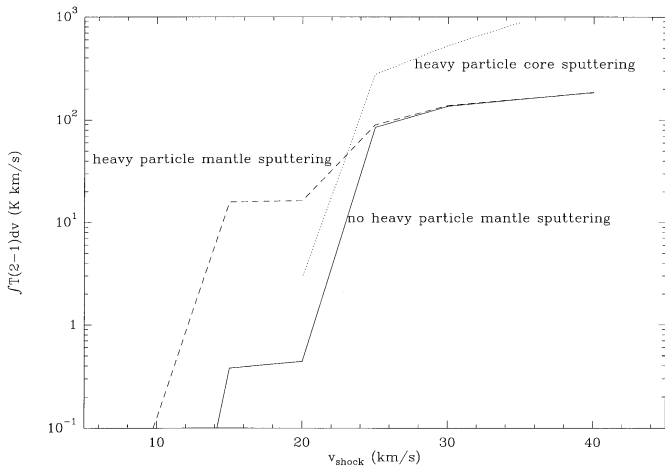


Fig. 8. Integrated intensity of SiO (2-1) as function of shock velocity for a density of 10^5 cm^{-3} . Models which include sputtering by heavy particles are denoted by broken lines.

velocities. This statement applies to erosion of the refractory grain cores and may also apply, to a lesser degree, to grain mantles. C-type shocks of modest speeds (15 km s^{-1}) might completely remove mantle material, which is then processed in the gas phase before being accreted in the cold, postshock gas. It follows that recurrent processing by C-shocks may have a significant influence on the composition of grain mantles. Processing of grains in the interstellar medium can have other consequences, including the formation of refractory organic mantles (Greenberg et al. 1993) which subsequently protect the core from erosion. If this is the case, the gas-phase SiO observed in outflows must originate from Si-bearing material in an outer, icy mantle. Similarly, the absence of SiO emission from certain outflow sources would be attributable to a low SiO abundance in this outer mantle.

Acknowledgements. This collaboration has been partially supported under the “Procope” programme. We are grateful to Eric Herbst for advice on reaction rates, to Rafael Bachiller for helpful discussions, and to David Field for his comments on an earlier version of our paper.

References

- Allen D.A., Burton M.G., 1993, *Nature*, 363, 54
 Anders E., Grevesse N., 1989, *Geochim. Cosmochim. Acta*, 53, 197
 Arthur N.L., Potzinger P., Reimann B., Steenbergen H.P., 1989, *J.Chem.Soc. Faraday Trans. 2*, 85, 1447
 Avery L.W., Chiao M., 1996, *ApJ*, 463, 642
 Bachiller R., Martin-Pintado J., Fuente A., 1991, *A&A*, 243, L21
 Bachiller R., Gomez-Gonzalez J., 1992, *A&A Rev.*, 3, 257
 Bachiller R., Liechti S., Walmsley C.M., Colomer F., 1995, *A&A*, 295, L51
 Barlow M.J., 1978, *MNRAS*, 183, 367
 Chandler C.J., De Pree C.G., 1995, *ApJ*, 455, L67
 Davis C.J. and Eisloffel J., 1995, *A&A*, 300, 851
 Draine B. T. 1994, *Astronomical Society of the Pacific Conference Series*, 58, 227
 Draine B.T., Roberge W.G., Dalgarno A., 1983, *ApJ*, 264, 485
 Dutrey A., Guilloteau S., Bachiller R., 1997, *A&A*, in press
 Eckstein W., 1991, *Computer Simulation of Ion-Solid Interactions*, Springer-Verlag, Berlin
 Elkin J.L., Armentrout P.B., 1984, *J.Phys.Chem.*, 88, 5454
 Field D., May P.W., Pineau des Forêts G., Flower D.R., 1996, *MNRAS*, in press
 Flower D.R., Pineau des Forêts G., 1994, *MNRAS*, 268, 724
 Flower D.R., Pineau des Forêts G., 1995, *MNRAS*, 275, 1049
 Flower D.R., Pineau des Forêts G., Walmsley C. M., 1995, *A&A*, 294, 815
 Flower D.R., Pineau des Forêts G., Field D., May P.W., 1996, *MNRAS*, 280, 447
 Gredel R., 1990 in “Molecular Astrophysics”, Hartquist T. W. ed, Cambridge University Press, Cambridge, p.305
 Greenberg J.M., Mendoza-Gomez C.X., de Groot M.S. & Breukers R. 1993, in “Dust and Chemistry in Astronomy”, Millar T.J. & Williams D.A. eds, IoP Publishing, Bristol, p. 271
 Haas M.R., Hollenbach D.J., Ericson E.F., 1986, *ApJ*, 301, L57
 Heck L., Flower D.R., Pineau des Forêts G., 1990, *Computer Phys. Comm.*, 58, 169
 Herbst E., Millar T.J., Wlodek S., Bohme D.K., 1989, *A&A*, 222, 205
 Jansen D.J., Spaans M., Hogerheijde M.R., van Dishoeck E.F., 1995, *A&A*, 303, 541
 Langer W.D., Glassgold A.E., 1990, *ApJ*, 352, 123
 Loh S.K., Jasinski J.M., 1991, *J.Chem.Phys.*, 95, 4914
 MacKay D.D.S., 1995, *MNRAS*, 274, 694
 MacKay D.D.S., 1996, *MNRAS* 278, 62
 Martin-Pintado J., Bachiller R., Fuente A., 1992, *A&A*, 254, 315
 McMullin J.P., Mundy L.G., Blake G.A., 1994, *ApJ*, 437, 305
 Merer A.J., Walmsley C.M., Churchwell E., 1982, *ApJ*, 256, 151
 Millar T.J., Rawlings J.M.C., Bennett A., Brown P.D., Charnley S.B., 1991, *A&AS*, 87, 585
 Millar T.J., Farquhar P.R.A., Willacy K., 1996, *A&AS*, 121, 139
 Mundy L.G., McMullin J., Blake G.A., 1995, *Ap. Space Sci.*, 224, 81
 Pineau des Forêts G., Roueff E., Flower D.R., 1990, *MNRAS*, 244, 668
 Pirronello V., 1993, in “Dust and Chemistry in Astronomy”, Millar T.J. and Williams D.A., eds, IoP Publishing, Bristol, p. 297
 Raga A.C., Cabrit S., Canto J., 1995, *MNRAS*, 273, 422
 Smith M.D., Brand P.W.J.L., 1990, *MNRAS*, 245, 108
 Sofia U.J., Cardelli J.A., Savage B.D., 1994, *ApJ*, 430, 650
 Tedds J.A., Brand P.W.J.L., Burton M.G., Chrysostomou A., Fernandes A.J.L., 1995, *Ap. Space Sci.*, 224, 139
 Turner B.E., 1991, *ApJ*, 376, 573
 Turner B.E., Chan K.W., Green S., Lubowich D.A., 1992, *ApJ*, 399, 114
 van Dishoeck E.F., Blake G.A., Draine B.T., Lunine J.I., 1993, in Levy E.H., Lunine J.I., Matthews M.S., eds, *Protostars and Planets III*, University of Arizona Press, p. 163
 Walmsley C.W., Schilke P., 1993, in “Dust and Chemistry in Astronomy”, Millar T.J. and Williams D.A., eds, IoP Publishing, Bristol, p. 37
 Whittet D.C.B., 1993, in “Dust and Chemistry in Astronomy”, Millar T.J. and Williams D.A., eds, IoP Publishing, Bristol, p. 9
 Wright M.C.H., Plambeck R.L., Mundy L.G., Looney L.W., 1995, *ApJ*, 455, L185
 Zhang Q., Ho P.T.P., Wright M.C.H., Wilner D.J., 1995, *ApJ*, 451, L71
 Ziegler J.F., Biersack J.P., Littmark U., 1985, *The Stopping Range of Ions in Solids*, vol. 1, in Ziegler J.F., ed, *The Stopping and Range of Ions in Matter*, Pergamon, New York
 Ziurys L.M., Friberg P., Irvine W.M., 1989, *ApJ*, 343, 201